Supporting Information

Versatile Colloidal Syntheses of Metal Chalcogenide Nanoparticles from Elemental Precursors using Amine-Thiol Chemistry

Swapnil D. Deshmukh,† Ryan G. Ellis,† Dwi S. Sutandar, David J. Rokke, and Rakesh Agrawal*

Davidson School of Chemical Engineering, Purdue University, West Lafayette, IN 47907, USA

† These authors contributed equally
*Corresponding author: agrawalr@purdue.edu

CIS Nanoparticle Synthesis:

CIS nanoparticles synthesized from various experimental methods including the hot injection, one pot heat up and microwave assisted solvothermal routes yield phase pure material without any presence of binary as can be seen from Raman analysis.

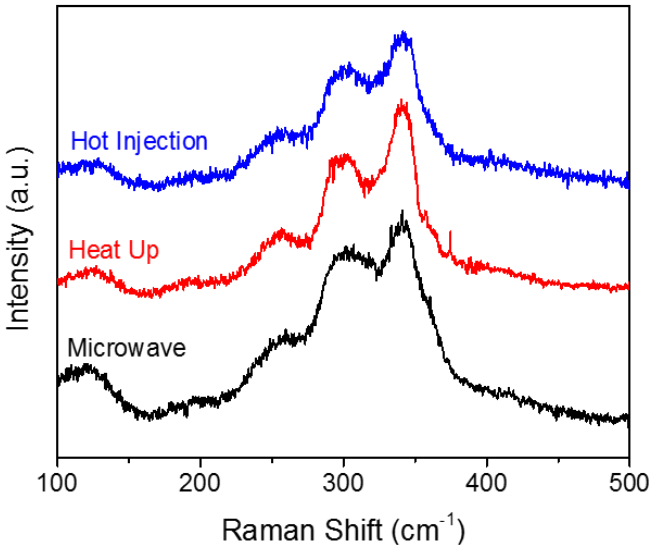

Figure S1. Raman spectroscopy analysis of CIS nanoparticles synthesized using hot injection, heat up and microwave assisted solvothermal reaction.

Effect of Thiol on Indium Sulfide Particles:

The evolution of amorphous trigonal indium sulfide to more crystalline tetragonal indium sulfide as a function of time could be related to the amount of thiol present in the reaction solution as a function of time. To verify this hypothesis, reactions were carried out for 60 min with varying quantity of thiol in the starting reaction solution. Although both the reactions resulted in mixture of amorphous trigonal indium sulfide and crystalline tetragonal indium sulfide, the reaction with reduced thiol quantity resulted in higher fraction of crystalline material as compare to reaction with excess thiol, supporting the hypothesis for thiol effect.

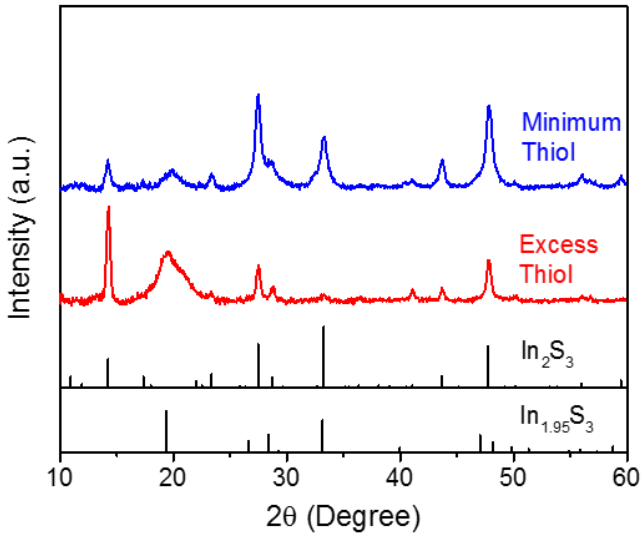

Figure S2. XRD analysis of indium sulfide particles synthesized using hot injection route for 60 min reactions with different thiol quantities. (Tetragonal phase In_2S_3 and trigonal phase $In_{1.95}S_3$ standards with ICSD collection code 151645 and 244280 respectively)

GC-MS Analysis of Indium Sulfide Reaction:

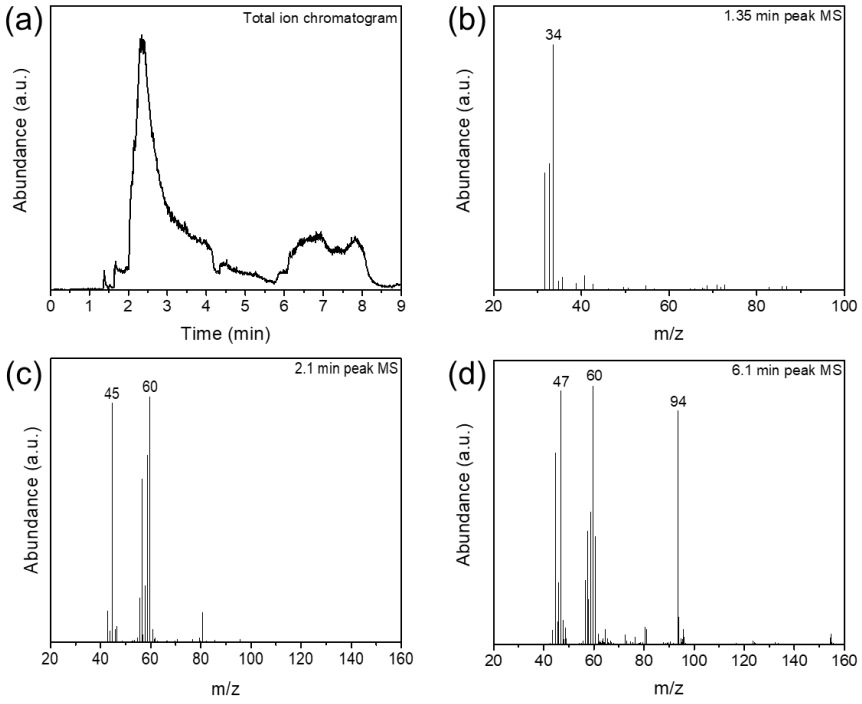

Figure S3. (a) Total ion chromatogram collected for indium-octylamine-ethanedithiol solution. Analyzed mass spectrum of isolated peak at elution time of (b) 1.35 min, (c) 2.1 min and (d) 6.1 min.

Cupper Sulfide Synthesis:

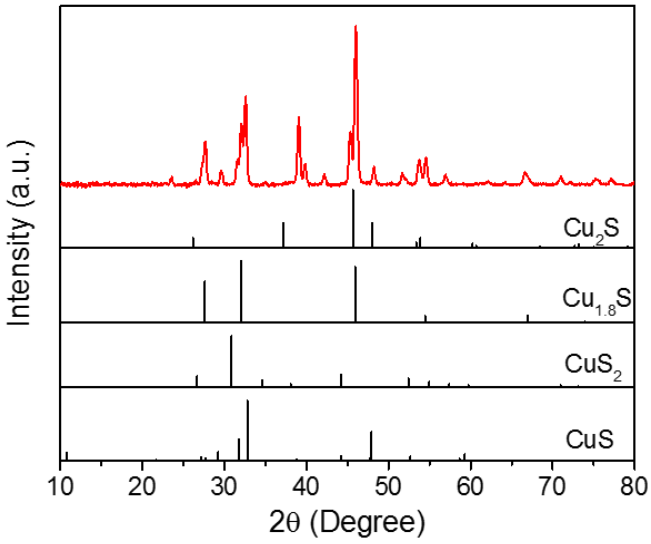

Figure S4. XRD analysis of nanoparticles synthesized via hot injection of Cu-PA-EDT ink in OLA showing formation of different phases of copper sulfides. (Cu_2S, $Cu_{1.8}S$, CuS_2 and CuS standards with ICSD collection code 200988, 95395, 100510 and 61793 respectively)

In-Ga Alloying:

Increasing gallium fraction in In-Ga sulfide resulted in reduced crystallinity of the particles as can be seen from XRD pattern below. The peak around 20° is shifted towards higher angles with increasing Ga fractions, suggesting possible incorporation of Ga into indium sulfide. The extent and uniformity of this alloying is further confirmed by performing STEM-EDS analysis on particles.

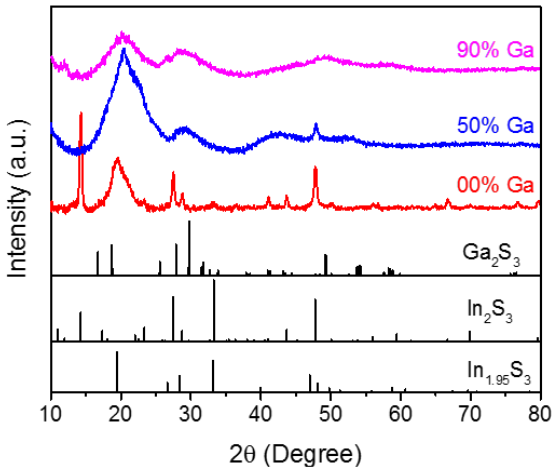

Figure S5. XRD analysis of indium-gallium sulfide particles synthesized using hot injection route with different gallium fractions. (Tetragonal phase In_2S_3, trigonal phase $In_{1.95}S_3$ and Ga_2S_3 standards with ICSD collection code 151645, 244280 and 409550 respectively)

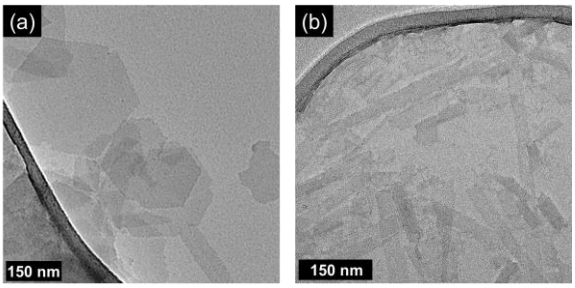

Figure S6. TEM images of indium-gallium sulfide nanostructures synthesized using hot injection with (a) 50% Ga and (b) 90% Ga fraction

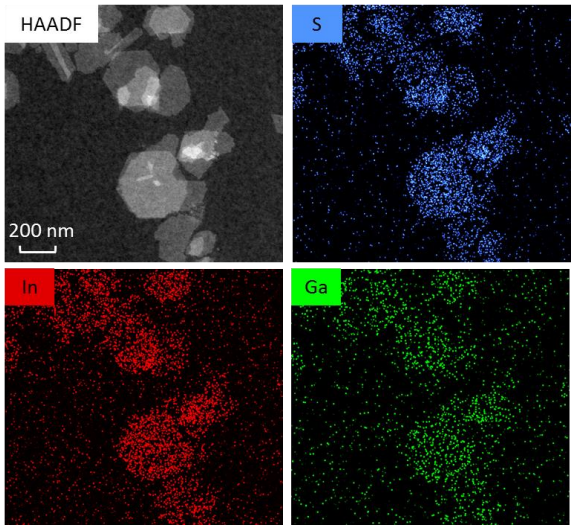

Figure S7. STEM-EDS elemental mapping of indium-gallium sulfide nanostructure containing 50% Ga showing uniformity of alloying within single particles as well as between multiple particles.

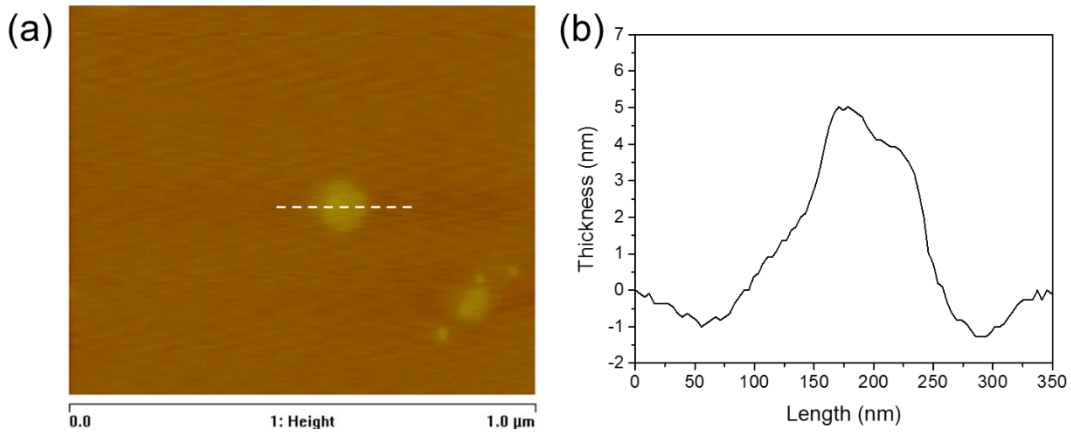

Figure S8. Atomic force microscopy on indium gallium sulfide nanostructure containing 50% Ga. (a) AFM image of the nanostructure (b) Plot showing thickness measurement of the nanostructure along the white dash line.

CIGS Nanoparticle Synthesis:

CIGS nanoparticle synthesis performed via one pot heat up route show absence of any binary formation (based on Raman analysis) for aliquots collected at various temperature during the course of heat up process. As can be seen from Figure S9, the A1 mode of CIS nanoparticles at 294 cm^{-1} shifts toward higher Raman shift of around 298 cm^{-1}, suggesting incorporation of Ga with increasing reaction temperature. Ga incorporation and elemental uniformity of CIGS particles is further confirmed via STEM-EDS analysis (Figure S10), while the particle surface is analyzed using FTIR (Figure 12a) and ^{1}H-NMR technique (Figure 12b), confirming the presence of oleylamine as ligand. The extra NMR peaks at δ of 4.03 ppm and 1.21 ppm corresponds to isopropyl alcohol used for washing nanoparticles while peak at δ of 4.54 ppm corresponds to ethylene carbonate, which was used as an internal 1H-NMR standard.

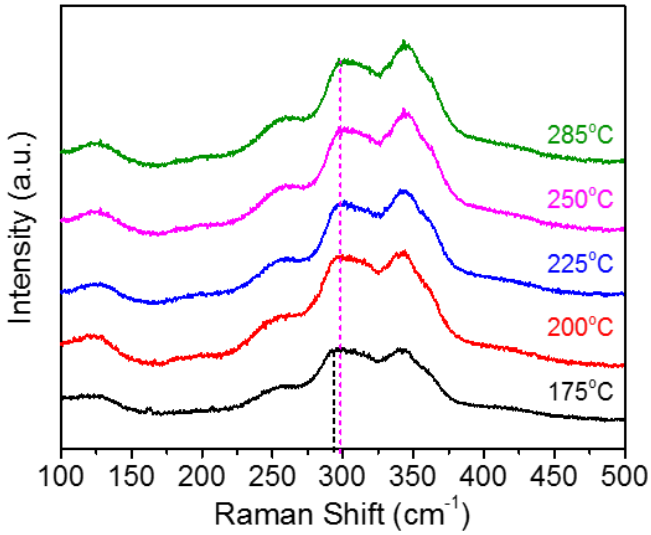

Figure S9. Raman analysis of CIGS nanoparticles during heat up process, showing incorporation of gallium in CIS structure as a function of temperature.

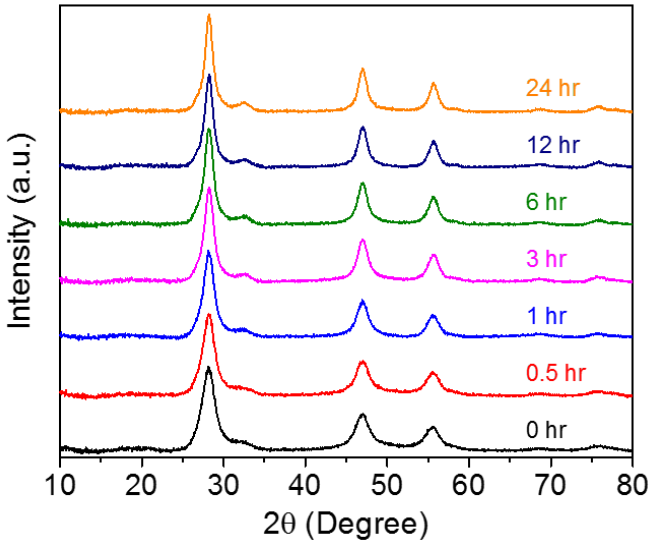

Figure S10. XRD analysis of CIGS nanoparticles synthesized using heat up route with different time aliquots showing reduced FWHM of peaks corresponding to increased particle size.

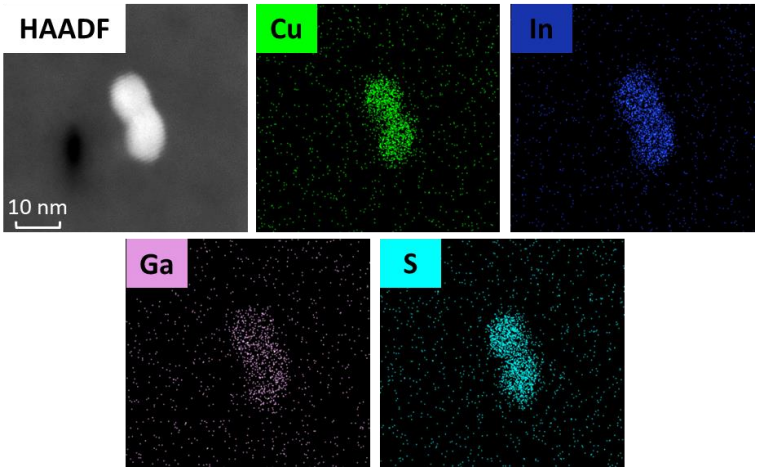

Figure S11. STEM-EDS elemental mapping of CIGS nanoparticles containing Ga/(Ga+In) of 0.3, showing elemental uniformity within single particles as well as between multiple particles.

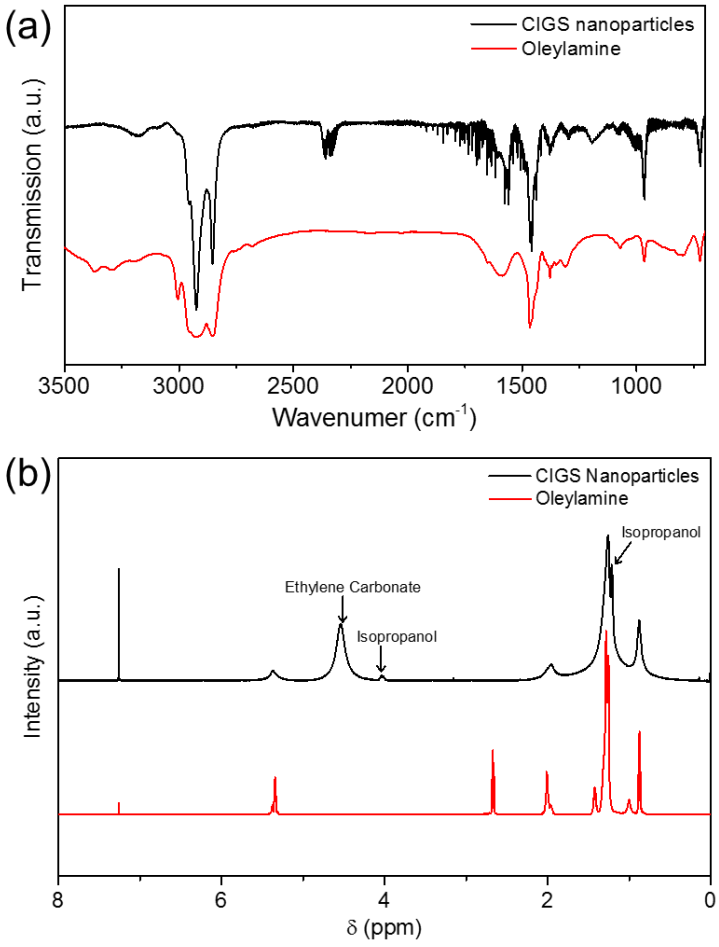

Figure S12. (a) FTIR analysis and (b) ^{1}H-NMR analysis of CIGS nanoparticles synthesized using heat up route confirming the presence of oleylamine on particle surface.

CISSe Nanoparticle Synthesis:

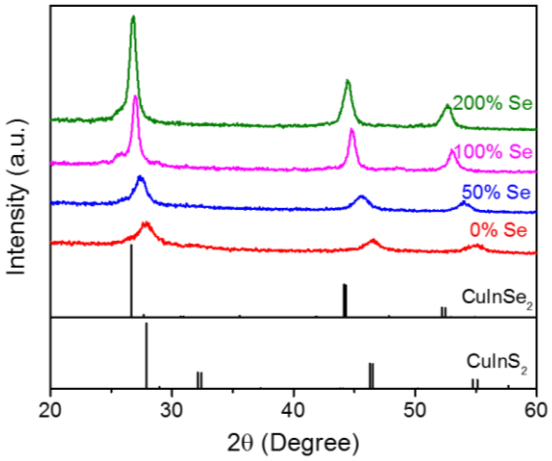

Figure S13. XRD analysis on CISSe nanoparticles as a function of Se quantity. (Chalcopyrite phase CIS and CISe standards with ICSD collection code 186714 and 73351 respectively)

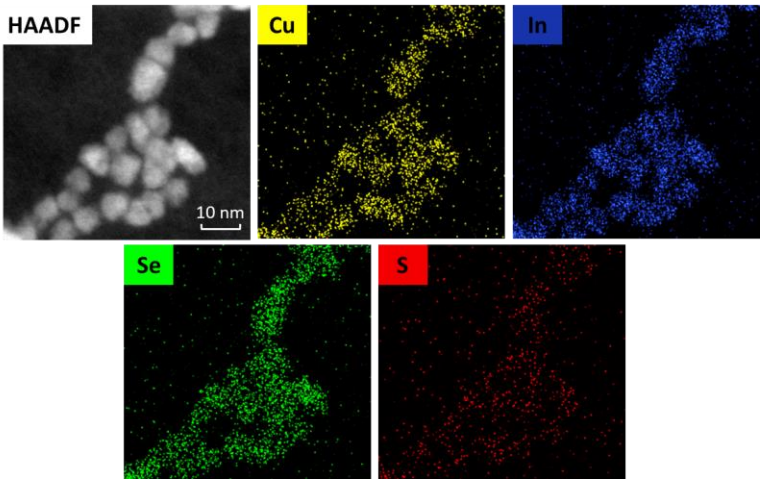

Figure S14. STEM-EDS elemental mapping of CISSe nanoparticles synthesized with reaction containing Se/(Cu+In) ratio of 2, showing elemental uniformity within single particles as well as between multiple particles.

CZTS Nanoparticle Synthesis suing heat up process:

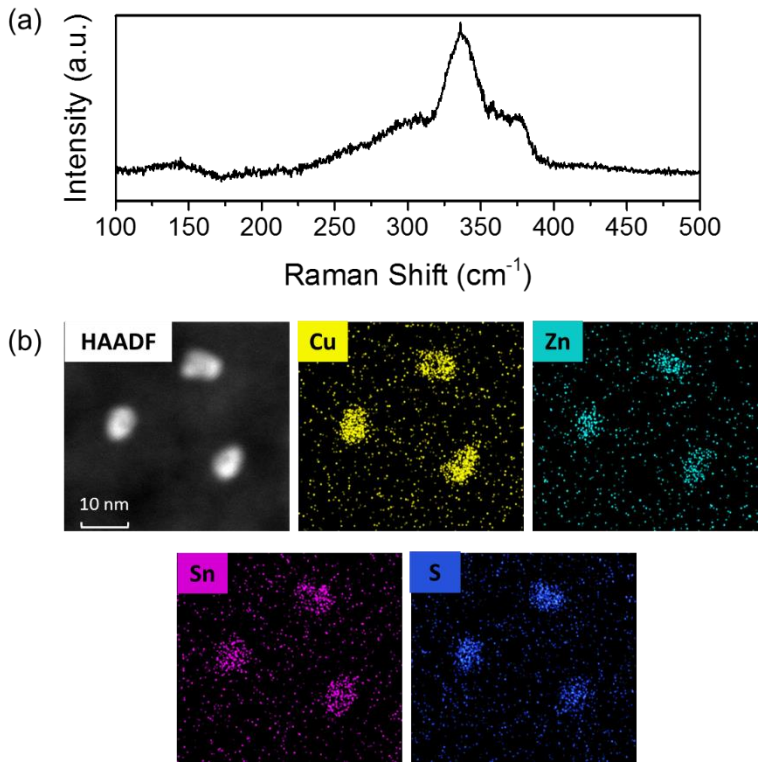

Figure S15. (a) Raman Spectroscopy analysis and (b) STEM-EDS elemental mapping of CZTS nanoparticles.

CIGS Nanoparticle Synthesis from Cu_2S Precursor:

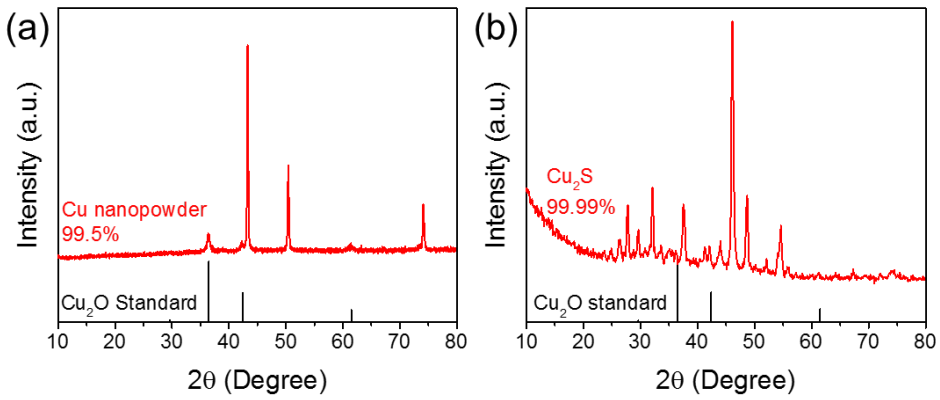

Figure S16. XRD analysis on as received (a) 99.5% pure Cu nanopowder showing presence of Cu_2O material and (b) 99.99% pure Cu_2S powder showing absence of Cu_2O materials.

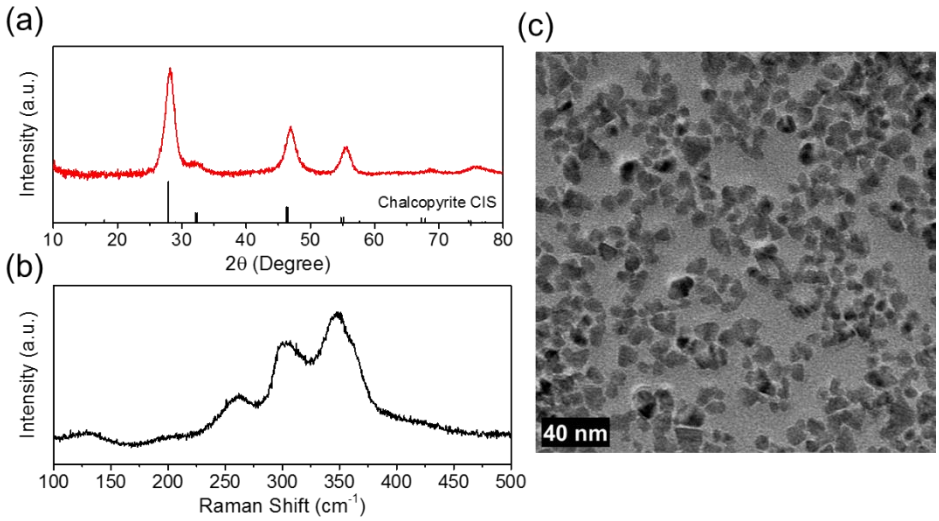

Figure S17. (a) XRD analysis, (b) Raman analysis and (c) TEM image of CIGS nanoparticles synthesized via heat up route using Cu_2S precursor instead of elemental Cu. (Chalcopyrite phase CIS standards with ICSD collection code 186714)

Wurtzite Phase CIGS Nanoparticle Synthesis:

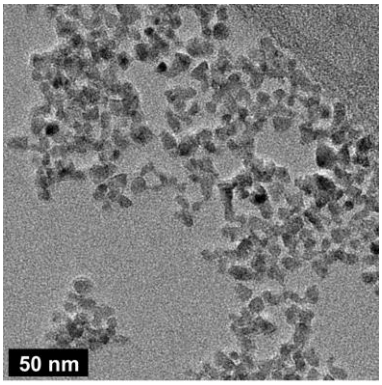

Figure S18. TEM images of wurtzite phase CIGS nanoparticles synthesized via heat up route with faster heating rate and 3 hours of reaction time